Available online at www.sciencedirect.com
ScienceDirect
Trans. Nonferrous Met. Soc. China 22(2012) 1786−1793
Transactions of Nonferrous Metals Society of China
www.tnmsc.cn

Corrosion behavior of micro-arc oxidation coating on AZ91D magnesium alloy in NaCl solutions with different concentrations

GUO Hui-xia[1,2], MA Ying[1], WANG Jing-song[1], WANG Yu-shun[1], DONG Hai-rong[1], HAO Yuan[1]

1. State Key Laboratory of Gansu Advanced Nonferrous Metal Materials, Lanzhou University of Technology, Lanzhou 730050, China;
2. Key Laboratory of Bioelectrochemistry and Environmental Analysis of Gansu Province, College of Chemistry and Chemical Engineering, Northwest Normal University, Lanzhou 730070, China

Received 5 July 2011; accepted 10 November 2011

Abstract: Ceramic oxide coatings were prepared on AZ91D magnesium alloys in alkaline silicate solution using micro-arc oxidation (MAO) technique. The corrosion behavior of MAO coating on AZ91D magnesium alloys in NaCl solutions with different concentrations (0.1%, 0.5%, 1.0%, 3.5% and 5.0% in mass fraction) was evaluated by electrochemical measurements and immersion tests. The results showed that the corrosion rate of the MAO coated AZ91D increased with increasing chloride ion concentration. The main form of corrosion failure was localized corrosion for the MAO coated AZ91D immersed in higher concentration NaCl solutions (1.0%, 3.5% and 5.0%), while it was general corrosion in dilute NaCl solutions (0.1% and 0.5%). Two different stages of the failure process of the MAO coated AZ91D could be identified: 1) occurrence of the metastable pits and 2) growth of the pits. Different equivalent circuits were also proposed based on the results of electrochemical impedance spectroscopy (EIS) for the MAO coated AZ91D immersed in different concentrations of NaCl solutions for 120 h.

Key words: micro-arc oxidation coating; AZ91D magnesium alloy; corrosion behavior; chloride ion concentration; electrochemical techniques

1 Introduction

Magnesium and its alloys have many favorable properties, such as high specific strength, high thermal conductivity, high damping characteristics and easy recycle, which make them attractive for applications in aerospace, automotive and electro-communication areas, etc [1,2]. However, magnesium and its alloys are highly susceptible to corrosion, which limits seriously their practical application, especially in some aggressive circumstance [2−4].

Suitable surface treatments can provide sufficient corrosion protection to the metal substrates. A number of surface treatment techniques have been developed for the protection of magnesium and its alloys, including chemical conversion coatings, electrochemical plating, anodizing, gas-phase deposition, organic coatings, sol−gel method, etc [1,5,6]. One of the most popular techniques, micro-arc oxidation (MAO), has been successfully applied to magnesium alloys against corrosion in recent years [7−10] based on the conventional anodic oxidation, and produces ceramic oxide coating with thickness of several tens of microns on the substrates. The MAO coatings on magnesium alloys are mainly composed of magnesium oxide and some of other electrolyte-borne elements ($Mg_3(PO_4)_2$, Mg_2SiO_4 or $MgAl_2O_4$ etc.) [8,10−12].

It is well known that chloride ion is one of the most important factors of the corrosion of magnesium alloys in many desirable applications. In general, magnesium alloys corrode at higher rates with increasing chloride ion concentration at all pH levels [13,14]. For MAO coating, CAI et al [8] studied corrosion and electrochemical performance of MAO coating on AZ91D magnesium alloy using step-down current method in phosphate and silicate electrolytes in 5.0% NaCl solution. GUO et al [9] studied the corrosion resistance of MAO coating on AZ31B magnesium alloy in alkaline silicate electrolyte in 3.5% NaCl solution. WANG et al [15]

Foundation item: Project (2007CB613700) supported by the National Basic Research Program of China; Project supported by Research Program of Excellent Scholars Studying Abroad of Ministry of Human Resources and Social Security, China
Corresponding author: MA Ying; Tel: +86-931-7971835; E-mail: mayingcn2008@163.com
DOI: 10.1016/S1003-6326(11)61388-5

evaluated corrosion resistance of MAO coating formed on SiC_w/AZ91D magnesium matrix composite using AC power supply in 3.5% NaCl solution. LIANG et al [16] investigated the electrochemical degradation of a silicate- and phosphate-based MAO coating on AM50 magnesium alloy using a pulsed DC power supply in NaCl solutions of different chloride ion concentrations (0.01, 0.1, 0.5 and 1 mol/L). However, up to now, there is a few research work to investigate the influence of chloride ion concentration on electrochemical corrosion behavior of MAO coating on AZ91D. In this work, the MAO coating was produced on AZ91D magnesium alloy using pulsed AC power supply in silicate-based electrolyte. The morphology and electrochemical corrosion behavior and durability of anti-corrosion of the MAO coating on AZ91D were investigated systemically in different concentrations of naturally aerated neutral NaCl solutions and the corrosion mechanisms were also elucidated.

2 Experimental

As one of the most widely used magnesium alloys, AZ91D magnesium alloy was used as the substrate material in this study. The chemical compositions of AZ91D are given in Table 1.

Table 1 Chemical composition of AZ91D magnesium alloy (mass fraction, %)

Al	Zn	Mn	Cu	Ni	Si	Mg
8.9	0.9	0.15	0.01	0.001	0.12	Balance

The samples for all tests were cut into cylinder with dimensions of *d*28 mm×10 mm and degreased with acetone in ultrasonic bath, then mechanically polished with 400 and 1200 grit emery papers, rinsed with distilled water and dried in warm air. The micro-oxidation process of the samples was conducted in alkaline silicate electrolyte solution which consisted of Na_2SiO_3 in distilled water with NaOH and KF. The AZ91D magnesium alloy samples and the stainless steel were used as the anode and cathode, respectively. Oxide coatings were produced at a constant voltage of 380 V for 30 min. The temperature of the electrolyte was kept nearly at 30 °C using a stirring and cooling system. The samples were rinsed in water and dried in hot air after MAO process was finished.

A MeF3 optical microscope (OM) and a JSM−6700F scanning electron microscope (SEM) were used to examine the surface morphology of the MAO coating. The corrosive media consisted of 0.1%, 0.5%, 1.0%, 3.5% and 5.0% (mass fraction) NaCl which were prepared using AR grade NaCl and distilled water. pH of the solution was around 6.8±0.2.

The electrochemical experiments were carried out using a conventional three-electrode cell with saturated calomel electrode (SCE) as a reference, a large area platinum electrode as a counter and the coated sample as working electrode (1 cm^2 exposed area). Potentio-dynamic polarization curves were obtained at a scanning rate of 0.5 mV/s using a CHI660C potentiostat controlled by PC. Electrochemical impedance spectroscopy (EIS) measurements were conducted with an amplitude of 10 mV over the frequency range of 500 kHz−10 mHz. The EIS measurements were performed with VMP2 multichannel potentiostat (PARC Corporation, USA). All tests were carried out at room temperature without stirring up to 120 h. Three tests for each sample were performed to ensure the results reasonable reproducibility. The data of EIS were fitted by software ZSimpWin 3.2.

3 Results and discussion

As shown in Fig. 1, a ceramic coating with thickness of (25±2) μm was obtained on AZ91D magnesium alloy by MAO process. Figure 1(a) reveals that the MAO coating on the AZ91D had a larger number of micro-pores and some micro-cracks on the surface. According to Refs. [17,18], the micro-pores were formed because of the molten oxide and gas bubbles throwing out in the MAO coating growth process. And the micro-cracks appeared due to the thermal stress from the

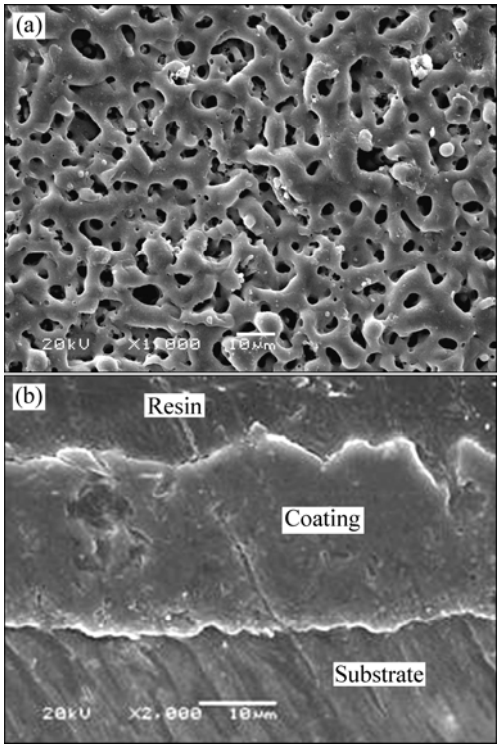

Fig. 1 SEM images of MAO coating on AZ91D surface (a) and cross section (b)

molten oxide fast solidified in the relatively cooling electrolyte. Figure 1(b) shows that the MAO coating had many irregular-shaped micro-pores, which did not inter-connect each other or passed through the whole film. The coating consisted mainly of MgO and Mg_2SiO_4 as investigated in our previous work [19].

3.1 Morphology of corroded surfaces

The OM morphologies of corroded surface of the MAO-coated AZ91D immersed in 0.5% and 5.0% NaCl solutions for 24 h are shown in Figs. 2(a) and (b). Many corrosion micro-pits were observed on both surfaces after 24 h immersion testing. With prolonging immersion time (120 h), however, the MAO-coated AZ91D samples immersed in different concentrations of NaCl solutions suffered from different extents of corrosion damage, as shown in Figs. 3(a) and (b). The exposed area of samples immersed in 0.1% and 0.5% NaCl solutions exhibited similar corrosion degradation. The corrosion was not significant and the corrosion damage enlarged gradually to cover the entire surface (Fig. 3(a)), and white acicular precipitations, most likely $Mg(OH)_2$, were fallen into the micro-pits/pores acting as protection barrier. On the other hand, the surface of the samples immersed in 5.0% NaCl solution presented to form larger, isolated, round etch pits with the diameter of about 0.2 mm (Fig. 3(b)). The corroded surface of sample immersed in 1.0% or 3.5% NaCl solution was similar to that immersed in 5.0%

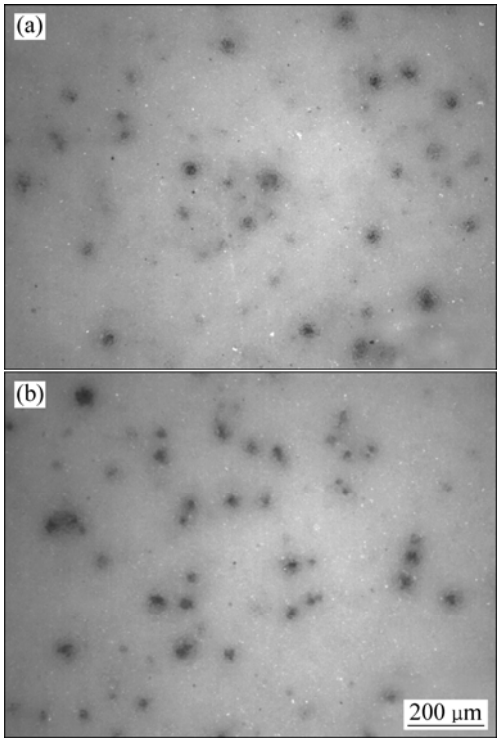

Fig. 2 OM morphologies of corroded surfaces of MAO-coated AZ91D magnesium alloys immersed in 0.5% (a) and 5.0% (b) NaCl solutions for 24 h

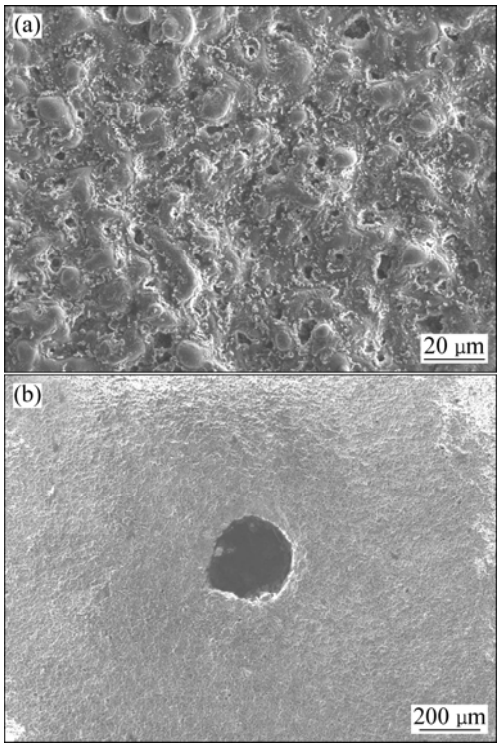

Fig. 3 SEM images of MAO coated AZ91D immersed in 0.5% (a) and 5.0% (b) NaCl solutions after 120 h

NaCl solution (morphologies not presented here), which indicated that the coating was damaged by typical localized corrosion in higher concentration NaCl solutions (1.0%, 3.5% and 5.0%). The micrographs after corrosion tests showed that the corrosion initiated from pits corrosion in NaCl solutions, which were defined as metastable pits. Finally, the corrosion attack was concentrated primarily in these regions at higher chloride ion concentrations (1.0%, 3.5% and 5.0%), while it spread to the other regions at lower chloride ion concentrations (0.1% and 0.5%).

3.2 Electrochemical measurements

3.2.1 Potentiodynamic polarization behavior

The potentiodynamic polarization curves of the MAO coated AZ91D samples in 0.1%, 1.0% and 5.0% NaCl solutions for different immersion time are presented in Fig. 4. The corrosion current density (J_{corr}) derived from polarization curves in all tested NaCl solutions by Tafel extrapolation method is summarized in Table 2.

It was found that the values of the corrosion current density at earlier immersion stage in all NaCl solutions were around 10^{-8} A/cm^2. It can also be seen that the J_{corr} values increased with immersion time when the MAO-coated AZ91D samples exposed to higher concentration NaCl solutions (3.5% and 5.0%). After immersion for 120 h, the J_{corr} values of the samples were almost three

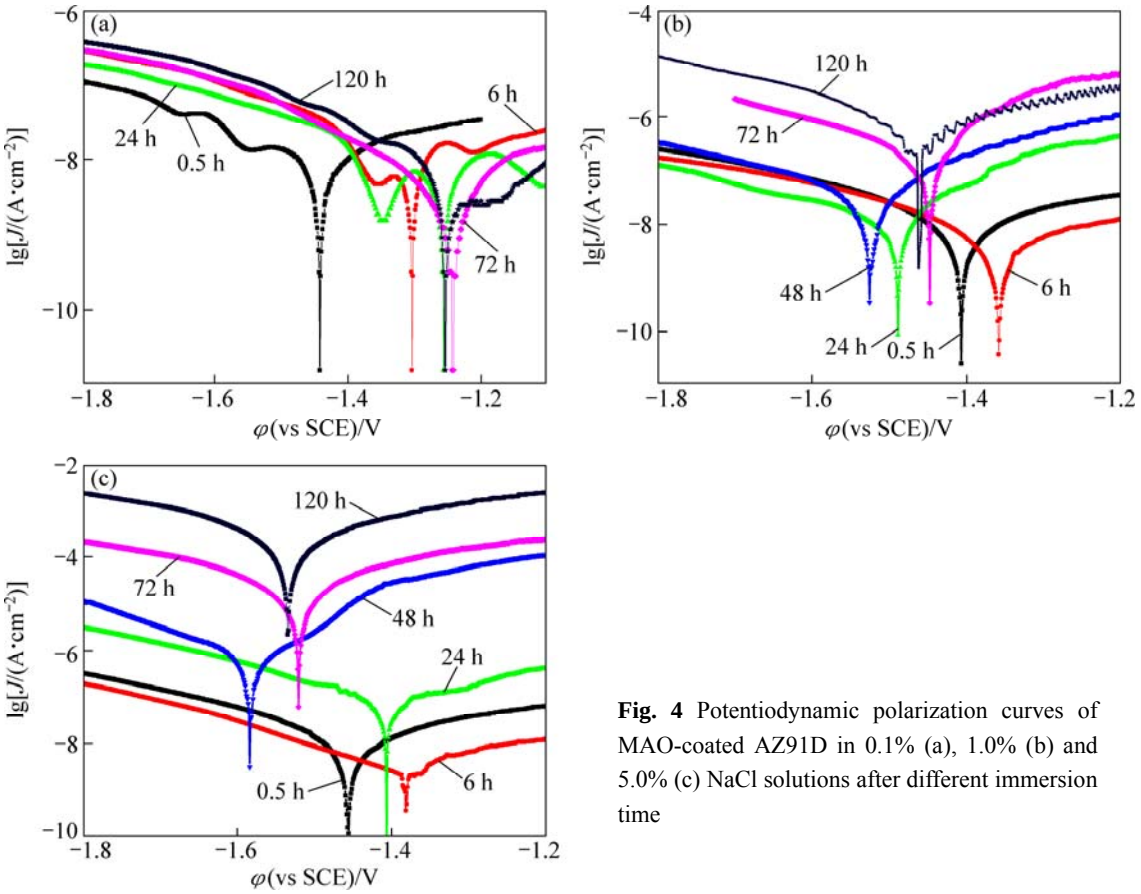

Fig. 4 Potentiodynamic polarization curves of MAO-coated AZ91D in 0.1% (a), 1.0% (b) and 5.0% (c) NaCl solutions after different immersion time

Table 2 Corrosion current densities (J_{corr}) of MAO coated AZ91D derived from polarization curves in different concentration NaCl solutions

Time/h	J/(A·cm^{-2})				
	0.1% NaCl	0.5% NaCl	1.0% NaCl	3.5% NaCl	5% NaCl
0.5	2.89×10^{-8}	2.69×10^{-9}	1.73×10^{-8}	6.64×10^{-8}	7.07×10^{-8}
6	1.98×10^{-8}	6.39×10^{-9}	9.74×10^{-9}	7.70×10^{-9}	1.14×10^{-9}
24	9.99×10^{-9}	3.83×10^{-9}	3.28×10^{-8}	8.68×10^{-8}	7.15×10^{-7}
48	7.24×10^{-9}	1.95×10^{-8}	6.40×10^{-8}	3.95×10^{-8}	2.01×10^{-6}
72	2.49×10^{-9}	2.94×10^{-9}	5.93×10^{-7}	9.45×10^{-7}	9.67×10^{-5}
96	1.33×10^{-9}	5.36×10^{-8}	2.48×10^{-7}	3.53×10^{-7}	1.85×10^{-5}
120	2.15×10^{-8}	2.75×10^{-8}	2.40×10^{-6}	5.32×10^{-6}	1.80×10^{-4}

orders higher compared with at earlier stage in 1.0% or 3.5% NaCl solution. While in 5.0% NaCl solution, the J_{corr} values increased to 10^{-4} A/cm^2, which implied that the sample had been destroyed. In the lower concentration NaCl solutions (0.1% or 0.5%), however, the J_{corr} values had no distinct changes with prolonging immersion time, indicating that lower concentration of Cl^- ion had no apparent effect on corrosion process and the MAO coating showed a better corrosion resistance in the relatively long-time exposures.

3.2.2 Electrochemical impedance spectroscopy (EIS)

The EIS technique is an effective method to understand the corrosion behavior of the metal and coated-metal system [16,17]. In this work, the impedance data as a function of immersion time were examined to reveal the corrosion resistant properties of the MAO-coated AZ91D magnesium alloy in different concentration NaCl solutions. Figure 5 shows the Bode plots of samples after different immersion time in NaCl solutions.

When the MAO-coated AZ91D samples were immersed in different concentration NaCl solutions, the EIS plots showed that the MAO coating provided similar corrosion protection properties in the initial corrosion

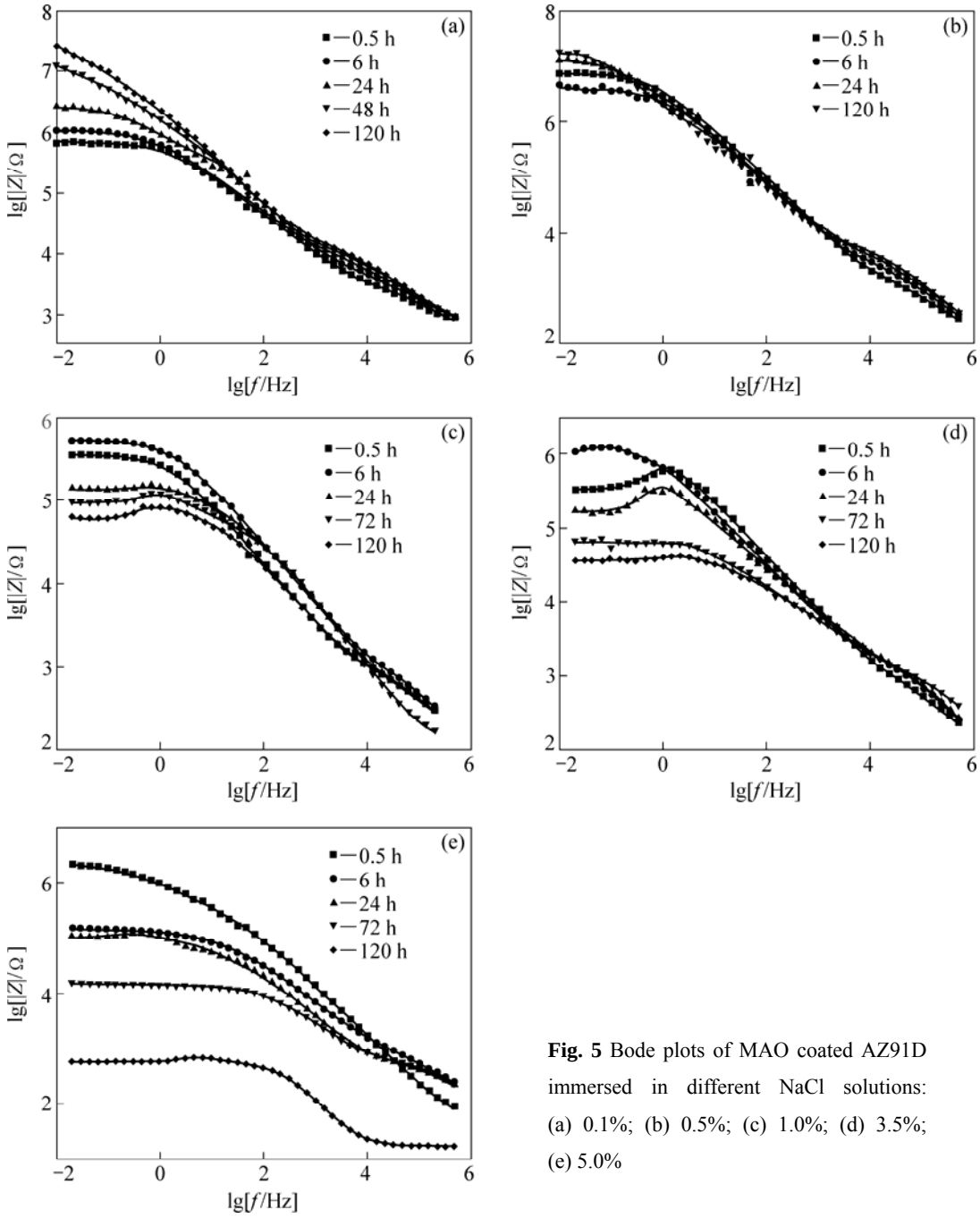

Fig. 5 Bode plots of MAO coated AZ91D immersed in different NaCl solutions: (a) 0.1%; (b) 0.5%; (c) 1.0%; (d) 3.5%; (e) 5.0%

process, consistent with the results of polarization. With prolonging the immersion time, different corrosion behaviors were displayed. According to the microstructural characteristics and the EIS behavior of the MAO-coated AZ91D samples, three equivalent circuits for fitting the EIS data obtained from different corrosive electrolytes are proposed in Fig. 6. Figure 6(a) shows an appropriate equivalent circuit for earlier stage of the MAO coating deterioration process (0.5−6 h) in NaCl solutions. Figures 6(b) and (c) are proposed to fit the latter stage of MAO coating on AZ91D immersed in dilute (0.1% and 0.5%) and higher concentration (1.0%, 3.5% and 5.0%) NaCl solutions, respectively.

In the equivalent circuits, the electrolyte resistance R_s is in series with the unit of the MAO-coated samples. R_1 presents the sum of resistance of outer porous layer in parallel with CPE_1 which is the constant phase element of the MAO coating exposed corrosion electrolyte. R_{ct} signs the charge–transfer resistance and parallels with CPE_2 which describes the properties of the inner barrier layer. R_m is the resistance of corrosion products and parallels with CPE_m, which is the surface of corrosion product/electrolyte interface. The inductance L is associated with the localized corrosion damage of sample and in series with R_{ct}. R_2 refers to the resistance of the insulating part of the inner barrier layer of the MAO

coating. The constant phase element (CPE) replaces the capacitance, which had been explained by dispersion effect. The EIS plots are fitted with these equivalent circuits and the fitting results are shown in Fig. 5 as solid lines.

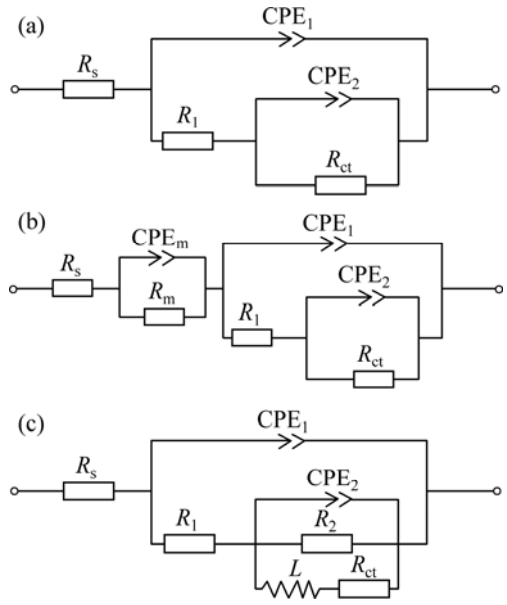

Fig. 6 Equivalent circuits for fitting impedance data of MAO coating in deterioration process of earlier stage (0.5−6 h) (a), latter immersion stage in NaCl solutions of 0.1% and 0.5% (b) and 1.0%, 3.5% and 5.0% (c)

R_{ct} is served as a parameter to characterize the corrosion rate. The values of lg R_{ct} for different immersion time from the equivalent circuit models are presented in Fig. 7. At the beginning of immersion, the value of R_{ct} was relatively low owing to penetration of the electrolyte into micro-pores of the MAO coating, which led to occurrence of a lot of metastable pits. During the subsequent immersion, NaCl solutions infiltrated through the defects in the outer porous layer and reached the interface of out/inner layer. Some soluble species and local oxide dissolution around the defects formed due to the existence of corrosive chloride ions adsorbed on many metastable pits. Because of the covering and blocking effect of these corrosion products, transfer of electrolyte was held back and the corrosion process of the MAO coating was slowed down. As a result, the value of R_{ct} increased. With prolonging immersion time, corrosive electrolyte reached the interface of inner layer/substrate and transferred in the MAO coating mainly by charge-transfer process with equably rate.

In dilute NaCl solutions (0.1% and 0.5%), the value of R_{ct} increased to relatively stable stage (around 10^7 $\Omega\cdot cm^2$). The Bode plots suggested that deterioration process of the MAO coating on AZ91D magnesium alloy

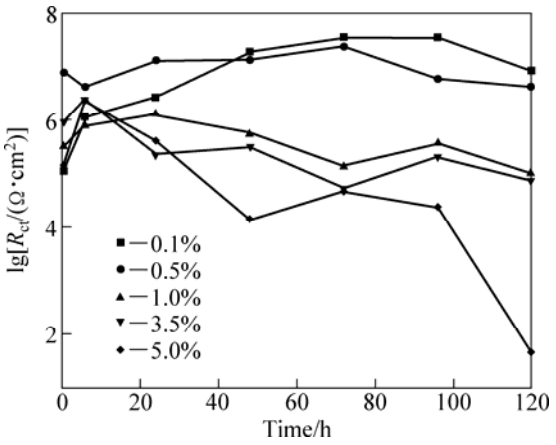

Fig. 7 R_{ct} of MAO coating on AZ910 immersed in NaCl solutions of different concentrations during test

immersed in dilute NaCl solutions progressed slowly. As a result, the MAO coating on AZ19D provided the longer-term corrosion protection for substrate in lower concentration of NaCl solution than in higher concentration of NaCl solution.

In higher concentration NaCl solution (1.0% and 3.5%), the value of R_{ct} decreased to a relatively stable value, about 10^5 $\Omega\cdot cm^2$. But in 5.0% NaCl solution, the value of R_{ct} decreased quickly, and after 120 h, it was less than 10^2 $\Omega\cdot cm^2$, which indicated that the MAO coating had lost the protection to magnesium alloy substrate.

3.3 Discussion

The fact that there is no pronounced corrosion damage in NaCl solutions for the MAO coated magnesium alloy is attributed to both the characteristics of the coating and the performance of corrosion electrolyte [20]. According to the previous work [19], the composition of the MAO coating on AZ19D consisted of MgO and Mg_2SiO_4. In this work, the compositions, microstructures and thickness of the MAO coating on AZ91D magnesium alloy produced with the same electronic parameters should be the same. Therefore, the influence of the characteristics of the MAO-coated AZ91D on the anti-corrosion resistance should be similar. Chloride ion is aggressive for magnesium alloy. Therefore, corrosion tests of the MAO-coated samples in different concentration neutral NaCl solutions were carried out to elucidate the corrosion mechanisms of coated magnesium alloy.

It was found that the corrosion of the MAO-coated AZ91D samples initiated from pitting (metastable pits), and then developed into localized corrosion in higher concentration NaCl solutions (1.0%, 3.5% and 5.0%) and general corrosion in dilute NaCl solutions(0.1% and 0.5%). Based on the corrosion results, the degradation of

the MAO coating could be divided into two stages: 1) Occurrence of the metastable pits. Due to the covering and blocking effect of the corrosion products, the degradation of the MAO coating was inhibited at this stage, which exhibited lower corrosion current density and higher charge-transfer resistance. 2) Growth of the pits. Degradation process of the MAO coating came into the steady state in this stage.

At the initial immersion stage, NaCl aqueous solutions were penetrated into the MAO coating and infiltrated through the micropores or microcracks in the out porous layer by diffusion and reached the interface of out/inner layer quickly. The dense inner layer played most important role in the anti-corrosion protection of the MAO coating on AZ91D magnesium alloy. As corrosive ions, chloride ions were absorbed preferentially and incorporated into the micropores. This led to local dissolution of the MAO coating around the defects. Whereafter a lot of metastable pits appeared. At the same time, the degradation products, such as $Mg(OH)_2$, owing to the hydration of MgO, sealed the metastable pits. It then acted as a protective barrier and prevented the exposure of magnesium alloy substrate.

Different second stages of the degradation of MAO coatings were revealed in different NaCl solutions. In the case of higher concentration of chloride ion solution (1.0%, 3.5% and 5.0%), the second stage was described that the incorporation of chloride ions into the coating replaced partial oxygen site [21] and led to formation of some soluble species, such as $MgCl_2$. Thus, it was possible for the coating to dissolute. The higher the concentration of Cl^- ions is, the more the replaced-O sites are, and the more the soluble species in the defects are. Anodic dissolution rate was higher than that of MgO hydration. The hydration products $Mg(OH)_2$ hardly filled the defects. When the corrosion products in the pores were moved into electrolytes, a concave pit left in the MAO coating on AZ91D. It was considered that dissolution may play an important role in initiation of pits of the MAO coating on AZ91D. And the development of the pits was in a highly occluded condition and controlled by diffusion of dissolved products within the pits. Once the pits had penetrated the MAO coating, several pits developed preferentially in the MAO coating and finally joined together to form a larger pit, which became macroscopic pores at last. The result was reflected in the impedance behaviour, which was indicated by the decrease of the impedance with increasing frequency in low-frequency range (in Figs. 5(c), (d), (e)). Figure 6(c) was used to fit the EIS spectra of MAO-coated AZ91D immersed in higher concentration (1.0%, 3.5% and 5.0%) NaCl solutions after localized corrosion initiation. It is an important step in pitting process of the incorporation of chloride ion into the coating. Therefore, Cl^- ion could accelerate the corrosion process of the MAO coating.

Regarding immersion process in dilute (0.1% and 0.5%) NaCl solutions for the MAO coating on AZ91D, the corrosive electrolyte filled with all micropores at first stage and reached the interface of outer /inner layer. The concentration of chloride ion was too low to stimulate active area to corrosion. The hydration of MgO became the main form of the MAO coating deterioration in these electrolytes. The corrosion on the whole surface area exposed to electrolyte was almost uniform. The intermediate product, $Mg(OH)_2$, was produced and adsorbed on the surface of the MAO coating. The intermediate products filled metastable pits and acted as a protection barrier suppressing the corrosion process due to the fact that the molar volume of $Mg(OH)_2$ is larger than that of MgO [16,17]. Therefore, the values of corrosion current density from the polarization and the resistance from the impedance of EIS measurements kept nearly the same during the immersion testing. After a long-term immersion (16−18 d), a layer with white acicular precipitations covered the whole surface and the sample became porous and gray in color. Corrosion evolution led to formation of a general corrosion layer with no preferential attack on the MAO coating. Figure 6(b) was used to fit the EIS spectra of the degradation of MAO coatings on AZ91D immersion in dilute NaCl solutions (0.1% and 0.5%) at the second stage. The elements stood for corrosion products layer (R_m and CPE_m) were in series with the unit of the MAO-coated AZ91D.

It is necessary to propound that if there exist through-going defects in evidence on MAO coating. These through-going defects would evolve as the active sites with higher corrosion rate of magnesium alloy substrate. Because of the lower resistance to transfer of electrolyte and corrosion products, the MAO coating on magnesium alloy would suffer from more severe localized damage during immersion in the NaCl solutions.

4 Conclusions

1) The MAO coating on AZ91D magnesium alloy was obtained by pulsed AC power source in alkaline silicate electrolyte. Electrochemical corrosion tests revealed that the corrosion damage for the MAO coating on AZ91D was dominated by pitting corrosion in higher concentrated NaCl solutions (1.0%, 3.5% and 5.0%) and by general corrosion in dilute NaCl solutions(0.1% and 0.5%).

2) Corrosion rates of the MAO-coated AZ91D magnesium alloy increased with increasing chloride ion concentration in NaCl solutions. It means that the MAO

coating on AZ91D magnesium alloy had a better corrosion protection in dilute NaCl solution than in higher concentration NaCl solution.

3) The degradation of the MAO coating can be identified with two different stages: the occurrence of the metastable pits and the growth of the pits.

References

[1] GRAY J E, LUAN B. Protective coatings on magnesium and its alloys—A critical review [J]. Journal of Alloys and Compounds, 2002, 336: 88−113.

[2] SONG Guang-ling. Corrosion and protection of magnesium alloys [M]. Beijng: Chemical Industry Press, 2006. (in Chinese)

[3] LIU L J, SCHLESINGER M. Corrosion of magnesium and its alloys [J]. Corrosion Science, 2009, 51: 1733−1737.

[4] SONG G, ATRENS A, WU X, ZHANG B. Corrosion behavior of AZ21, AZ501 and AZ91 in sodium chloride [J]. Corrosion Science, 1998, 40: 1769−1791.

[5] HUO H, LI Y, WANG F. Corrosion of AZ91D magnesium alloy with a chemical conversion coating and electroless nickel layer [J]. Corrosion Science, 2004, 46: 1467−1477.

[6] GALIO A F, LAMAKA S V, ZHELUDKEVICH M L, DICK L F P, MÜLLER I L, FERREIRA M G S. Inhibitor-doped sol-gel coatings for corrosion protection of magnesium alloy AZ31 [J]. Surface and Coatings Technology, 2010, 204: 1479−1486.

[7] ARRABAL R, MATYKINA E, HASHIMOTO T, SKELDON P, THOMPSON G E. Characterization of AC PEO coatings on magnesium alloys [J]. Surface and Coatings Technology, 2009, 203: 2207−2220.

[8] CAI Q, WANG L, WEI B, LIU Q. Electrochemical performance of microarc oxidation films formed on AZ91D magnesium alloy in silicate and phosphate electrolytes [J]. Surface and Coatings Technology, 2006, 200: 3727−3733.

[9] GUO H, AN M, XU S, HUO H. Microarc oxidation of corrosion resistant ceramic coating on a magnesium alloy [J]. Materials Letters, 2006, 60: 1538−1541.

[10] LIANG J, HU L, HAO J. Characterization of microarc oxidation coatings formed on AM60B magnesium alloy in silicate and phosphate electrolytes [J]. Applied Surface Science, 2007, 253: 4490−4496.

[11] LIANG J, GUO B, TIAN J, LIU H, ZHOU J, XU T. Effect of potassium fluoride in electrolytic solution on the structure and properties of microarc oxidation coatings on magnesium alloy [J]. Applied Surface Science, 2005, 252: 345−351.

[12] ARRABAL R, MATYKINA E, VIEJO F, SKELDON P, THOMPSON G E. Corrosion resistance of WE43 and AZ91D magnesium alloys with phosphate PEO coatings [J]. Corrosion Science, 2008, 50: 1744−1752.

[13] SONG G, ATRENS A, JOHN D S, WU X, NAIRN J. The anodic dissolution of magnesium in chloride and sulphate solutions [J]. Corrosion Science, 1997, 39: 1981−2004.

[14] ALTUN H, SEN S. Studies on the influence of chloride ion concentration and pH on the corrosion and electrochemical behavior of AZ63 magnesium alloy [J]. Materials & Design, 2004, 25: 637−643.

[15] WANG Y Q, ZHENG M Y, WU K. Microarc oxidation coating formed on SiCw/AZ91 magnesium matrix composite and its corrosion resistance [J]. Materials Letters, 2005, 59: 1727−1731.

[16] LIANG J, SRINIVASAN P B, BLAWERT C, DIETZEL W. Influence of chloride ion concentration on the electrochemical corrosion behavior of plasma electrolytic oxidation coated AM50 magnesium alloy [J]. Electrochimica Acta, 2010, 55: 6802−6811.

[17] DUAN H, DU K, YAN C, WANG F. Electrochemical corrosion behavior of composite coatings of sealed MAO film on magnesium alloy AZ91D [J]. Electrochimica Acta, 2006, 51: 2898−2908.

[18] LIANG J, SRINIVASAN P B, BLAWERT C, DIETZEL W. Comparison of electrochemical corrosion behavior of MgO and ZrO_2 coatings on AM50 magnesium alloy formed by plasma electrolytic oxidation [J]. Corrosion Science, 2009, 51: 2483−2492.

[19] LV W L, CHEN T J, MA Y, XU W J, YANG J, HAO Y. Effects of increase extent of voltage on wear and corrosion resistance of micro-arc oxidation coatings on AZ91D alloy [J]. Transactions of Nonferrous Metals Society of China, 2008, 18: 354−360.

[20] SHI Z, SONG G, ATRENS A. The corrosion performance of anodised magnesium alloys [J]. Corrosion Science, 2006, 48: 3531−3546.

[21] XUE R, QIAN Y Y, LIU K K, JIANG X X, ZHU J J, ZHANG J R. Nano-pit corrosion of the tabs in aluminum electrolytic capacitor: Polarization characteristics of the tabs in ethyleneglycol-borate solution with chloride ions [J]. Corrosion Science, 2008, 50: 2779−2784.

AZ91D 镁合金微弧氧化膜在不同浓度 NaCl 溶液中的腐蚀行为

郭惠霞[1,2]，马 颖[1]，王劲松[1]，王宇顺[1]，董海荣[1]，郝 远[1]

1. 兰州理工大学 有色金属新材料国家重点实验室培育基地，兰州 730050；

2. 西北师范大学 化学化工学院，甘肃省生物电化学与环境分析重点实验室，兰州 730070

摘 要：采用微弧氧化技术(MAO)在镁合金 AZ91D 表面制备微弧氧化陶瓷膜。利用电化学技术和浸泡实验研究该镁合金试样在不同浓度(0.1%，0.5%，1.0%，3.5%和 5.0%，质量分数) NaCl 溶液中的腐蚀行为。结果表明，试样的腐蚀速率随着氯离子浓度的升高而增大。在较高浓度(1.0%，3.5%和 5.0%)的 NaCl 溶液中的主要腐蚀形式是点蚀，而在较低浓度(0.1%和 0.5%)中是全面腐蚀。腐蚀过程可以分为两个阶段：亚稳态蚀点的出现和蚀点的生长。根据腐蚀过程中阻抗谱的特点，对镁合金微弧氧化膜试样在不同浓度 NaCl 溶液中浸泡 120 h 提出了不同的等效电路来模拟其腐蚀行为。

关键字：微弧氧化膜；AZ91D 镁合金；腐蚀行为；氯离子浓度；电化学技术

(Edited by YANG Hua)